

The ORCA Option for KM3NeT

Ulrich F. Katz for the KM3NeT Collaboration^{*†}

Friedrich-Alexander University of Erlangen-Nürnberg,

Erlangen Centre for Astroparticle Physics

E-mail: katz@physik.uni-erlangen.de

It has recently been suggested that the neutrino mass hierarchy can be experimentally determined from the oscillation pattern of atmospheric neutrinos passing through the Earth by measuring the two-dimensional arrival pattern of neutrinos in energy and zenith angle, in the energy regime of about 3–20 GeV. ORCA (Oscillation Research with Cosmics in the Abyss) is a study addressing the feasibility of such a measurement employing the deep-sea neutrino telescope technology developed for the KM3NeT project. In the following, the underlying physics and resulting experimental signatures will be discussed and some aspects of the ongoing simulation studies presented. A preliminary sensitivity estimate derived from a simplified study strongly indicates that an exposure of at least 20 Mton-years will be required to arrive at conclusive results.

XV Workshop on Neutrino Telescopes,

11-15 March 2013

Venice, Italy

^{*}Speaker.

[†]www.km3net.org

1. Neutrino oscillations and mass hierarchy

All current experimental information on neutrino oscillations can be described correctly within a theoretical framework containing three neutrino types which have different sets of flavour and mass eigenstates and different, hence non-zero masses. The flavour eigenstates, denoted ν_α with $\alpha = e, \mu, \tau$, are relevant for weak interactions, i.e. neutrino generation and reactions. The mass eigenstates (ν_i with masses m_i , $i = 1, 2, 3$) govern neutrino propagation through space-time.

The relation between flavour and mass eigenstates is given by the unitary Pontecorvo-Maki-Nakagawa-Sakata matrix $U_{\alpha i}$,

$$|\nu_\alpha\rangle = \sum_{i=1,2,3} U_{\alpha i} |\nu_i\rangle. \quad (1.1)$$

A commonly used parameterisation of U in terms of three mixing angles $\theta_{12}, \theta_{13}, \theta_{23}$ and one complex phase $e^{i\delta}$ is given by

$$U = \begin{pmatrix} 1 & 0 & 0 \\ 0 & c_{23} & s_{23} \\ 0 & -s_{23} & c_{23} \end{pmatrix} \cdot \begin{pmatrix} c_{13} & 0 & s_{13}e^{-i\delta} \\ 0 & 1 & 0 \\ -s_{13}e^{i\delta} & 0 & c_{13} \end{pmatrix} \cdot \begin{pmatrix} c_{12} & s_{12} & 0 \\ -s_{12} & c_{12} & 0 \\ 0 & 0 & 1 \end{pmatrix} \quad (1.2)$$

with $s_{ij} = \sin \theta_{ij}$ and $c_{ij} = \cos \theta_{ij}$. Two additional complex phases appear in eq. (1.2) if neutrinos are Majorana particles. Since the Dirac or Majorana nature of neutrinos is unknown and these phases are of no significance for the following discussion, they are omitted here.

If the mixing angles and the mass-squared differences $\Delta m_{ij}^2 = m_i^2 - m_j^2$ are non-zero, neutrino oscillations are a necessary consequence. For propagation along a path length L through vacuum the probability $P_{\alpha \rightarrow \beta}$ for a flavour state α to turn into flavour state β can be calculated analytically from

$$P_{\alpha \rightarrow \beta} = e^{ipL} \sum_{i=1,2,3} U_{\beta i} e^{-iE_i t} U_{i\alpha}^\dagger \quad (1.3)$$

where t the propagation time, p the momentum and $E_i = \sqrt{p^2 + m_i^2}$ the energy of mass eigenstate i . Since the neutrino mass is experimentally constrained to $m_i \lesssim 2 \text{ eV}$, we can assume $p \gg m_i$ in the following, hence in particular $t = L/c$ and $E_i = p + m_i^2/(2p)$. The complex phase $e^{i\delta}$ introduces a CP-violating difference between oscillation probabilities of neutrinos and antineutrinos. Neglecting these and other sub-leading terms¹, the resulting $e \leftrightarrow \mu$ oscillation probability can be written as

$$P_{e \rightarrow \mu} = P_{\mu \rightarrow e} = \sin^2 \theta_{23} \sin^2(2\theta_{13}) \sin^2 \left(\frac{\Delta_{13} L}{2} \right) \quad (1.4)$$

with $\Delta_{13} = \Delta m_{13}^2/(2E_\nu)$. A characteristic feature of vacuum oscillations is that they do not depend on the signs of Δm_{ij}^2 , i.e. they do not provide information on the mass ordering of the ν_i .

For propagation in matter, e.g. through Sun or Earth, the oscillation pattern is modified by the fact that ν_e have elastic interaction modes with electrons that are not possible for other flavour eigenstates: In addition to the t -channel exchange of a Z boson (possible for all neutrino flavours), elastic $\nu_e e$ ($\bar{\nu}_e e$) scattering can proceed through u (s) channel exchange of a W boson. As a result,

¹Note that the identification of sub-leading terms requires the knowledge of the mixing angles (see below).

the forward scattering amplitude and hence the index of refraction for ν_e is different from the other flavours. This effect is described quantitatively by an extra term in the Hamiltonian of the \vec{V}_e ,

$$A = \pm\sqrt{2}G_F N_e \quad \text{with} \quad \begin{cases} + & \text{for } \nu_e \\ - & \text{for } \bar{\nu}_e, \end{cases} \quad (1.5)$$

where G_F is the Fermi constant and N_e the number density of electrons in the matter. The presence of this term modifies eq. (1.4) to

$$P_{e \rightarrow \mu}^M = P_{\mu \rightarrow e}^M = \sin^2 \theta_{23} \sin^2(2\theta_{13}^{\text{eff}}) \sin^2\left(\frac{\Delta_{13}^{\text{eff}} L}{2}\right) \quad (1.6)$$

$$\sin^2(2\theta_{13}^{\text{eff}}) = \sin^2(2\theta_{13}) \cdot \frac{\Delta_{13}^2}{(\Delta_{13}^{\text{eff}})^2} \quad (1.7)$$

$$\Delta_{13}^{\text{eff}} = \sqrt{[\Delta_{13} \cos(2\theta_{13}) - A]^2 + \Delta_{13}^2 \sin^2(2\theta_{13})}. \quad (1.8)$$

Note that via eq. (1.8) the oscillation pattern now depends on the sign of Δ_{13} and is different for neutrinos and antineutrinos; in particular, we have

$$P_{e \rightarrow \mu}^M(\nu, \pm\Delta m_{13}^2) = P_{e \rightarrow \mu}^M(\bar{\nu}, \mp\Delta m_{13}^2). \quad (1.9)$$

From measurements of atmospheric, solar, reactor and accelerator neutrinos the parameters of neutrino oscillations are meanwhile rather precisely known (for details see [1]). The mixing angles are roughly given by $\sin \theta_{23} = \pi/4$, $\sin \theta_{12} = \pi/5.4$ and $\sin \theta_{13} = \pi/20$, where the latter was the last to be measured about two years ago. The mass differences are about $\Delta m_{12}^2 = 7.5 \times 10^{-5} \text{ eV}^2$ and $|\Delta m_{23}^2| = 2.4 \times 10^{-3} \text{ eV}^2$ (the third mass difference is not an independent quantity). The sign of Δm_{12}^2 is known due to matter effects in neutrino propagation through the Sun. The sign of Δm_{23}^2 , however, is as yet unknown, leaving two scenarios for neutrino mass ordering, denoted by *normal hierarchy (NH)* and *inverted hierarchy (IH)*, respectively (see Fig. 1).

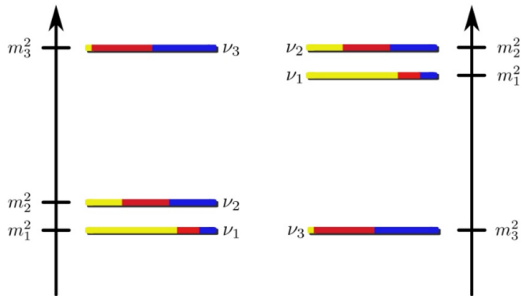


Figure 1. Graphic representation of neutrino masses and mixing, for the normal hierarchy (left) and the inverted hierarchy (right). The yellow (red, blue) fractions of the lines indicate the ν_e (ν_μ , ν_τ) contents of the mass eigenstates.

A measurement of the neutrino mass hierarchy – as one of the fundamental parameters of the Standard Model of particle physics – is an important goal in itself. Beyond that, it would be important for easing the experimental determination of the CP-violating phase $e^{i\delta}$ in future experiments, and it could help in interpreting cosmological data and their dependence on the neutrino sector.

2. Measuring the neutrino mass hierarchy with atmospheric neutrinos

Atmospheric neutrinos are mostly generated in π , K and μ decays in extended air showers initiated by cosmic ray interactions with nuclei in the Earth atmosphere. In the atmospheric neutrino

flux [2], ν_μ and $\bar{\nu}_\mu$ dominate over ν_e and $\bar{\nu}_e$, and at energies beyond a few GeV muon neutrinos are slightly more abundant than muon antineutrinos.

In order to exploit a matter-induced oscillation effect to distinguish NH and IH, $\bar{\nu}_e$ must be involved. This is in particular the case for $\nu_\mu \leftrightarrow \nu_e$ transitions which can be assessed experimentally through measuring the atmospheric ν_μ and/or the ν_e event rates as functions of E_ν and the oscillation path length, $L = |2R_E \cos \vartheta|$ (R_E being the Earth radius and ϑ the zenith angle). The effect is strongest for $\sqrt{2}G_F N_e = \Delta_{13} \cos(2\theta_{13})$, where according to eqs. (1.7) and (1.8) $\sin^2(2\theta_{13}^{\text{eff}}) = 1$. This condition is met for $E_\nu \approx 30 \text{ GeV} / \rho [\text{g cm}^{-3}]$, where ρ is the matter mass density. Typical Earth densities are between 3 g cm^{-3} for the crust and 13 g cm^{-3} for the inner core (see Fig. 2), implying that the relevant neutrino energy regime is a few to about 20 GeV.

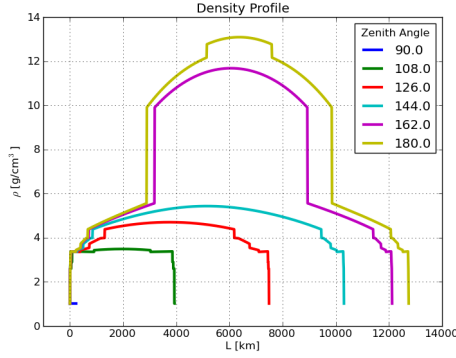


Figure 2. Density profiles of the Earth as traversed by neutrinos entering the detector under different zenith angles. Zenith angles of 180° (90°) correspond to vertically upward (horizontal) neutrino directions. The density data are taken from the *Preliminary Reference Earth Model (PREM)* [3].

Since experiments with sufficient target mass to measure precisely the atmospheric neutrino flux in this energy range are too large to be magnetised, the charge of the lepton ℓ produced in the relevant reactions, $\bar{\nu}_\ell N \rightarrow \ell^\pm X$ (N being the target nucleon and X the hadron final-state system), cannot be measured and hence a distinction between neutrinos and antineutrinos is impossible. Nevertheless, a measurable net effect remains due to the fact that the νN and $\bar{\nu} N$ cross sections differ significantly in the relevant energy regime, $\sigma(\nu N) \approx 2\sigma(\bar{\nu} N)$.

The measurement described above has e.g. been suggested in [4] where the expected differences between event numbers in the NH and IH scenarios have been calculated in bins of E_ν and ϑ . The resulting “pseudo-significances”, $(N^{\text{NH}} - N^{\text{IH}}) / \sqrt{N^{\text{NH}}}$, are shown in Fig. 3 for $\ell = \mu$ (left) and $\ell = e$ (right). Even though these plots do not include any experimental smearing and assume an unrealistically optimistic effective detector volume, it becomes obvious that a significant measurement might be possible also under more realistic conditions. Note that some of the patterns are caused by the inhomogeneous Earth density profile (parametric resonances).

3. The ORCA feasibility study

ORCA stands for *Oscillation research with Cosmics in the Abyss* and denotes the approach to perform the measurements discussed in Section 2 with a deep-sea neutrino telescope in the Mediterranean Sea, using the technology developed for the KM3NeT project [5, 6]. Neutrino telescopes [7] consist of large 3-dimensional arrays of photo-sensors in transparent environments that register the Cherenkov light of charged secondary particles emerging from neutrino reactions. From the arrival time of the Cherenkov photons (nanosecond precision) and the positions of the sensors (uncertainty about 10 cm), the direction and energy of the incoming neutrino can be reconstructed.

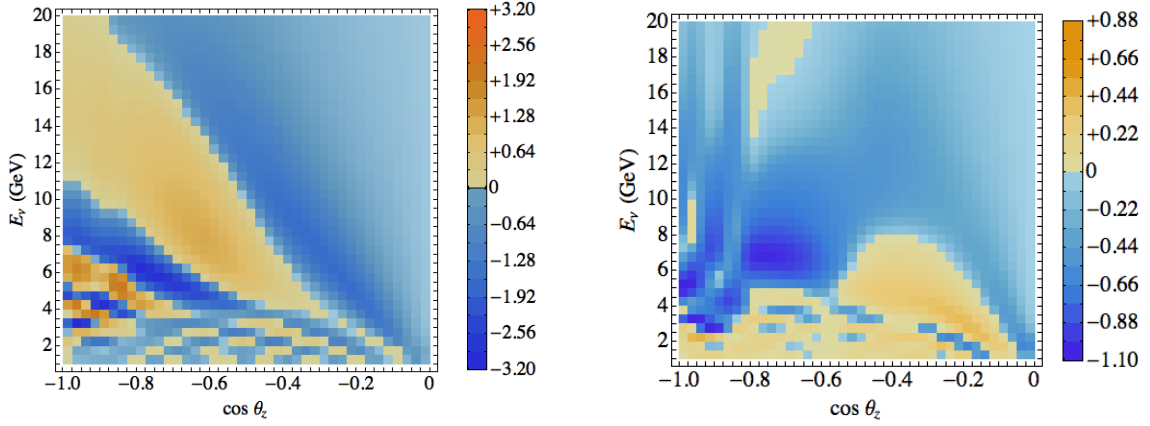


Figure 3. Pseudo-significances $(N^{\text{NH}} - N^{\text{IH}})/\sqrt{N^{\text{NH}}}$ per (E_ν, ϑ) bin, for ν_μ (left) and ν_e events (right), after one year of data taking and an assumed effective volume increasing from 2 to 20 Mton for neutrino energies from 2 to 20 GeV. Perfect experimental resolution and efficiency was assumed. Plots taken from [4].

A detailed feasibility study addressing the prospects of measuring the neutrino mass hierarchy with a deep-sea neutrino telescope is being prepared by the KM3NeT collaboration². For this study, an example detector configuration was chosen with 50 strings, carrying 20 digital optical modules (DOMs) each (see Fig. 4); each DOM is equipped with 31 3-inch photomultipliers. The distance between neighbouring strings is 20 m, the vertical distance between adjacent DOMs is 6 m. The instrumented volume is $1.75 \times 10^6 \text{ m}^3$, corresponding to about 1.8 Mton of sea water. The detector is assumed to be installed at a water depth of 3.5 km. Apart from the geometrical configuration (and the corresponding cable lengths), the detector design has been adopted “as is” from KM3NeT. The technical feasibility of the selected configuration appears likely but will have to be verified by engineering studies before embarking on a possible future proposal.

The following performance issues are addressed in detailed simulation studies:

- What are the trigger and event selection efficiencies?
- How can neutrino events in the relevant energy range be reconstructed and which resolutions in E_ν and ϑ can be achieved?
- How can the backgrounds be controlled?
- How and how efficiently can the different event classes (in particular ν_μ and ν_e) be separated?
- What are the systematic effects and how can they be controlled?

Answers to these question are meanwhile known, even though some are still partial or preliminary. A consistent picture emerges, indicating that a measurement could be possible but will require an exposure (effective volume times running time) of roughly $20 \text{ Mton} \cdot \text{year}$ for a significance of $3\text{--}5\sigma$. A selection of findings leading to this conclusion is presented in the following.

²A similar study is also pursued in the context of the IceCube neutrino telescope in the deep ice of the South Pole: *Precision IceCube Next-Generation Upgrade, PINGU* [8, 9].

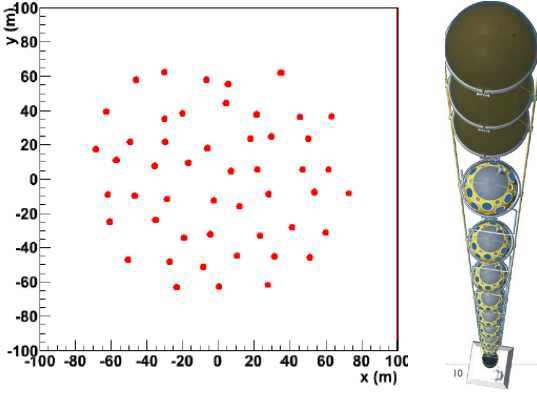


Figure 4. Footprint of the 50 detector strings assumed in the ORCA feasibility study (left) and artist's view of one string (right). Note that the string drawing is not to scale.

We start by discussing reactions of the type $\nu_\mu N \rightarrow \mu X$ (“muon channel”) with up-going neutrino, i.e. zenith angle $\vartheta > 90^\circ$. As in KM3NeT, all photomultiplier signals above a noise threshold (typically 0.3 photo-electrons) are sent to shore and processed by an online event filter there. We find that the filter conditions can be adjusted such that the random background from potassium-40 decays is almost completely suppressed and the event selection efficiency exceeds 50% (90%) for neutrino energies above 3 GeV (6 GeV). This result is not surprising as the muon tracks at the relevant neutrino energies are rather short and thus the coincidence time windows can be kept small.

The event reconstruction mostly uses the information of the muon track, which has a length of about 5 m per GeV of muon energy. The event reconstruction yields the muon track length and direction, the vertex position and a quality parameter, Λ ; currently, no attempt is made to reconstruct the hadronic shower. Well-reconstructed events are selected by cutting on Λ and requiring the reconstructed vertex to be inside the instrumented volume. For the resulting event sample, the vertex is reconstructed with an average deviation from the true value of less than 5 m (2.5 m) for neutrino energies above 3 GeV (15 GeV). In Fig. 5 the effective volume and the direction reconstruction precision are shown as functions of the neutrino energy. The event selection is almost fully efficient for $E_\nu > 5$ GeV, and the mismatch between reconstructed muon and true neutrino direction is completely dominated by the intrinsic contribution, except at lowest energies.

The energy estimate is currently based on the reconstructed muon track length. This approach is problematic in cases where the muon leaves the detector volume (“semi-contained events”), or in events in which a large fraction of E_ν goes into the hadronic system X (high $y = (E_\nu - E_\mu)/E_\nu$). The reconstructed muon energy, E_μ^R , is shown in Fig. 6 as a function of the true E_μ , for contained and for semi-contained events. The neutrino energy is estimated by multiplying E_μ^R with a correction function $f(E_\mu^R)$ derived from Monte Carlo simulation. The resulting reconstructed neutrino energy, E_ν^R , has a median offset from E_ν of about 1 GeV at $E_\nu \lesssim 6$ GeV, rising to 3 GeV (10 GeV) for $E_\nu = 10$ GeV (20 GeV). Note that for a Gaussian resolution function the quoted median corresponds to 0.67σ . An improvement of the energy resolution is expected from properly taking into account the hadronic system X ; this is work in progress and results are not yet available. In the following we will therefore make generic assumptions on the energy resolution.

The main source of background are atmospheric muons, i.e. those that are generated in extended air showers in the upper hemisphere, penetrate to the detector and are reconstructed as up-going. Even though the probability for such misreconstruction is tiny, the resulting background

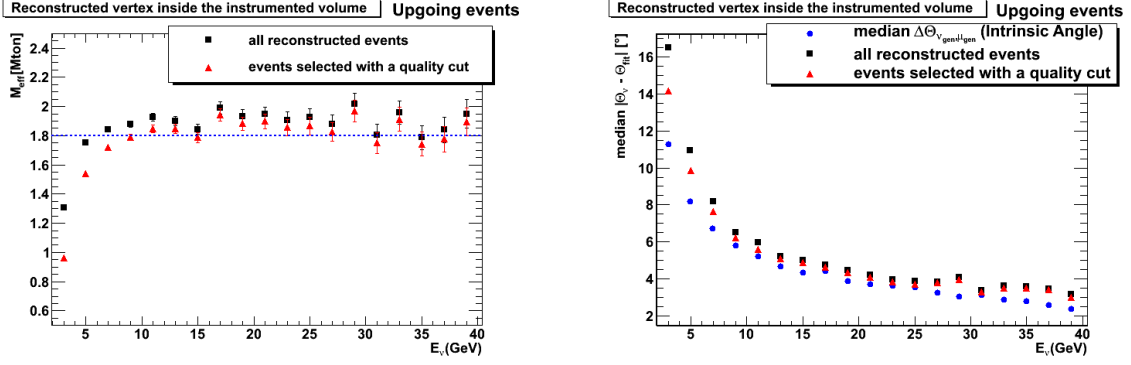


Figure 5. Left: Effective volume of the ORCA detector as a function of E_ν , for all reconstructed and for the selected events. The instrumented volume is indicated by the dashed line. The volume is given in units of mass, using the density of sea water. Right: Average angular mismatch between true neutrino and reconstructed muon direction as a function of E_ν , for the same two event classes. The blue symbols show the mismatch between the true ν and μ directions (“intrinsic angle”).

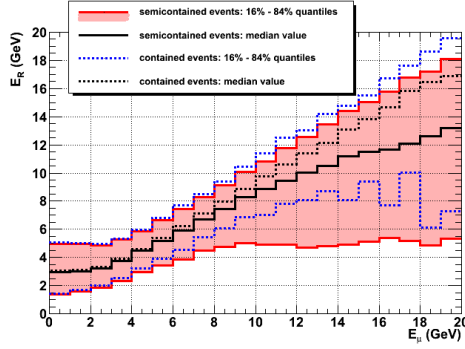


Figure 6. Muon energy reconstructed from track length, E_R , versus true muon energy. The solid black line (pink area) show the averages and the 1σ quantiles for semi-contained events. The black (blue) dashed lines indicate the same quantities for contained events.

can be large since atmospheric muon events are roughly 6 orders of magnitude more frequent than neutrino events. In absence of a surrounding detector volume to be used as veto against atmospheric muons (as in the case of PINGU and IceCube), this background source must be removed at the event selection/reconstruction level. It has been found that this is well possible by applying cuts on Λ (see above), on the uncertainty of the reconstructed muon direction, β , as well as on the reconstructed vertex position. Figure 7 shows the distribution of the reconstructed vertex position in the horizontal plane after Λ and β cuts, for neutrinos and atmospheric muons. A clean separation of these event samples is possible and the remaining background level can be adjusted to 10% or even 1% without a prohibitive loss of signal events.

Building on the results presented above, a simplified significance analysis was performed by generating a large number of “pseudo-experiments” (PEs), i.e. simulated experimental measurements of event distributions in the plane of reconstructed E_ν and ϑ . These PEs cover a range of assumed measurement durations and are generated under the following assumptions:

- the neutrino interactions are generated inside the instrumented volume and at least 15 photo-multiplier hits are required;
- the true muon direction is used for ϑ (cf. Fig. 5) and a Gaussian uncertainty on E_ν between 10% and 30% is applied;

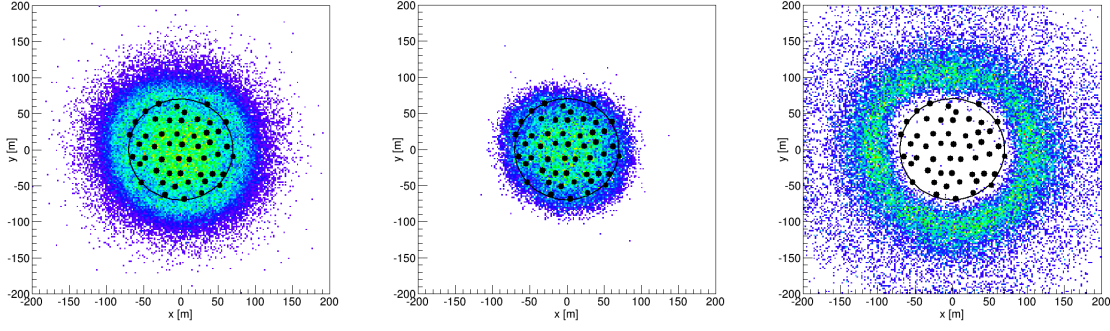


Figure 7. Reconstructed vertex positions (coloured points) in the horizontal plane for all events reconstructed as up-going, after Λ and β cuts, for all simulated neutrino events (left), the neutrino events with true $E_\nu < 20\text{GeV}$ (middle) and for atmospheric muons (right). The detector footprint is also indicated. The black circles denote a possible fiducial volume cut. Note that the atmospheric muons are through-going and do not have a real vertex in the vicinity of the positions indicated.

- no backgrounds from atmospheric muons or neutrino reactions other than in the muon channel are considered;
- for each PE, NH or IH is assumed and a set of oscillation parameters ($\theta_{ij}, \Delta m_{ij}^2, \delta$, see Sect. 1) is selected according to Gaussian distributions given by the current world averages and uncertainties of these parameters, but neglecting correlations between them.

Each PE is analysed by performing a log-likelihood fit with the oscillation parameters as free parameters and assuming both hierarchies in turn. The maximum likelihoods \mathcal{L} resulting from these fits are used to calculate the parameter

$$Q = \sum_{\text{bins}} \log [\mathcal{L}(\text{PE data}|\text{NH})] - \sum_{\text{bins}} \log [\mathcal{L}(\text{PE data}|\text{IH})], \quad (3.1)$$

which is used to quantify the separability of the NH and IH hypotheses. The main conclusions are:

1. ORCA will significantly constrain Δm_{23}^2 and θ_{23} beyond their current precision but is rather insensitive to the other oscillation parameters; in particular, no substantial sensitivity to the CP-violating phase $e^{i\delta}$ is found.
2. In turn, the current experimental errors on Δm_{23}^2 and θ_{23} induce a systematic uncertainty, in particular as the patterns in the (E_ν, ϑ) plane caused by the variation of these parameters within their error bounds is similar to the NH/IH difference to be assessed (see Fig. 8). Note that this systematic uncertainty is automatically accounted for in the statistical analysis.
3. The distribution of the Q values of all PEs is investigated to calculate the significance of a mass hierarchy measurement as a function of the exposure. The Q distributions are shown in Fig. 9 (left); the significance, calculated from the distance and the widths of Gaussians fitted to the NH and IH distributions, is presented in Fig. 9 (right).

Since the assumptions made are realistic, but on the optimistic side, the resulting significances can be taken as a “best-case scenario” for an analysis of the muon channel only. They are in

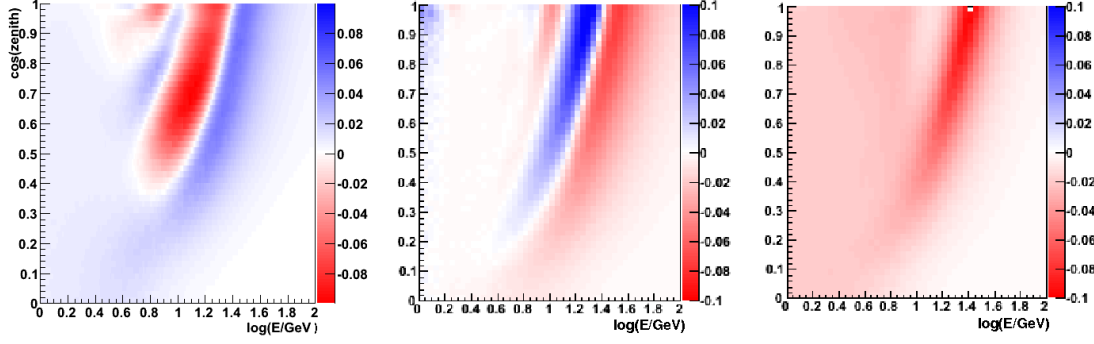


Figure 8. Expected relative differences between event numbers in the NH and IH scenarios (left) and relative event number modifications for varying Δm_{23}^2 (middle) or θ_{23} (right), respectively.

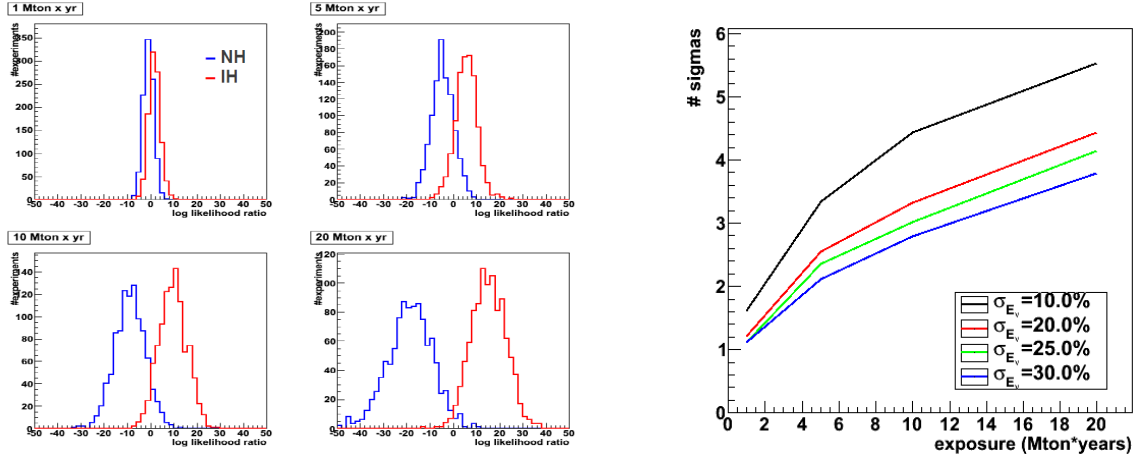


Figure 9. Left: Q distributions for the NH (blue) and IH (red) scenarios, for exposures between 1 Mton · year and 20 Mton · year, for a Gaussian E_ν resolution with width 25%. Right: Resulting significances as a function of exposure, for different Gaussian energy resolutions assumed.

fact compatible with the results of a parametric study reported in [10]. We have studied in detail sources of systematic uncertainty beyond that induced by the errors on the oscillation parameters. It is found that those caused by the Earth density profiles and the flux shape of the atmospheric neutrinos are small. A future improvement in the muon channel might be possible by using the reconstructed y values for $\nu/\bar{\nu}$ separation, as suggested in [11].

It has recently been realised that the electron channel, i.e. reactions of the type $\nu_e N \rightarrow eX$, can contribute substantially to the significance of a neutrino mass hierarchy measurement. In fact the unsmeared NH/IH pattern (Fig. 3, right) is less striking than in the muon channel, but it is also less affected by experimental resolution effects. To make best use of this additional analysis handle, muon and electron events have to be distinguished. It has been shown that in ORCA, for $E_\nu \gtrsim 5$ GeV, more than 80% of all muon and electron events can be classified correctly using Random Decision Forest techniques. The resulting overall performance of ORCA is still under investigation.

A possible future option could be a long-baseline neutrino beam targeted on ORCA. Such a beam could e.g. be produced in Protvino, as discussed in [12].

4. Conclusions and Outlook

The deep-sea neutrino telescope technology developed in the KM3NeT project could be used to construct a densely instrumented detector to investigate the neutrino mass hierarchy by measuring the energy and zenith distribution of atmospheric neutrinos. Using the muon channel alone, a 3–5 σ significance may be in reach for an overall exposure of 20 Mton-year; including the electron channel could significantly improve the prospects.

Acknowledgments

The author wishes to thank the organisers for a truly inspiring meeting and for patiently accepting this contribution long after the deadline.

References

- [1] J. Beringer et al. (Particle Data Group), *Review of Particle Physics, section 13: Neutrino mass, mixing, and oscillations*. Phys. Rev. **D 86**, 010001 (2012). 2013 partial update for the 2014 edition available on <http://pdg.lbl.gov/2013/reviews/rpp2013-rev-neutrino-mixing.pdf>.
- [2] T.K. Gaisser and M. Honda, *Flux of atmospheric neutrinos*. Ann. Rev. Nucl. Part. Sci. **52**, 153 (2002), [arXiv:hep-ph/0203272].
- [3] A.M. Dziewonski and D.L. Anderson, *Preliminary reference Earth model*. Physics of Earth and Planet Interiors **25**, 297 (1981).
- [4] E.Kh. Akhmedov, S. Razzaque and A.Yu. Smirnov, *Mass hierarchy, 2-3 mixing and CP-phase with huge atmospheric neutrino detectors*. JHEP **1302**, 082 (2013), [arXiv:1205.7071v6 [hep-ph]].
Erratum *ibid*, 1307 (2013) 026.
- [5] P. Sapienza, for the KM3NeT Collaboration, *KM3NeT perspectives*, 2014. These proceedings.
- [6] KM3NeT web page, available on <http://www.km3net.org>.
- [7] U.F. Katz and Ch. Spiering, *High-energy neutrino astrophysics: Status and perspectives* **67**, 651 (2012), [arXiv:1111.0507 [astro-ph.HE]].
- [8] M.G. Aartsen et al., IceCube-PINGU Collaboration, *Letter of Intent: The Precision IceCube Next Generation Upgrade (PINGU)*. Preprint arXiv:1401.2046 [physics.ins-det], 2014.
- [9] M. Kowalski, for the IceCube-PINGU Collaboration, *PINGU: Precision IceCube Next-Generation Upgrade*, 2014. These proceedings.
- [10] W. Winter, *Neutrino mass hierarchy determination with IceCube-PINGU*. Phys. Rev. **D 88**, 013013 (2013), [arXiv:1305.5539 [hep-ph]].
- [11] M. Ribordy and A.Yu. Smirnov, *Improving the neutrino mass hierarchy identification with inelasticity measurement in PINGU and ORCA*. Phys. Rev. **D 87**, 113007 (2013), [arXiv:1303.0758 [hep-ph]].
- [12] J. Brunner, *Counting electrons to probe the neutrino mass hierarchy*. Preprint arXiv:1304.6230 [hep-ex], 2013.